49th IEEE Conference on Decision and Control
December 15-17, 2010
Hilton Atlanta Hotel, Atlanta, GA, USA

Extremum Seeking Micro-Thermal-Fluid Control for Active Two-Phase Microelectronics Cooling

TieJun Zhang, John T. Wen, Agung Julius, Yoav Peles, Michael K. Jensen
Center for Automation Technologies and Systems
Rensselaer Polytechnic Institute, Troy, NY 12180, USA
{zhangt6,wenj,juliua2,pelesy,jensem}@rpi.edu

Abstract— **To address increasing power densities in high power electronic devices, microchannel systems operating in the two-phase regime have been explored in recent years for high heat flux cooling applications. However, flow and thermal oscillations, frequently present in two-phase microchannel cooling, may severely compromise the cooling performance and system integrity. This paper considers the thermal-fluid control of a microchannel evaporator by regulating the inlet flow rate using a pump. The control objective is two-fold: stabilize the fluid flow and maintain a low evaporator wall temperature. The first objective is easily achieved with a proportional feedback of flow acceleration. The second objective is more challenging as the achievable wall temperature depends on the heat transfer coefficient which in turn depends on the flow rate and heat load and is typically not well characterized. In this paper, we present an adaptive extremum seeking control law which first uses the wall temperature measurement to estimate the heat transfer coefficient, and then adjusts the flow rate to maximize this estimate. Simulation results demonstrate the efficacy of the proposed scheme.**

I. Introduction

Effective and efficient thermal management of next-generation electromagnetic systems, defense radars, all-electric ships/vehicles, and supercomputers is attracting more attention due to the high power-density bottleneck and high energy efficiency requirement [1], [2]. The peak heat dissipation rate of next-generation electronic systems is expected to exceed 1000 W/cm^2 [3], [4], while the surface temperature of most microelectronics has to be maintained below 85 °C for reliability [4]. For such high transient heat flux applications, conventional cooling solutions are inadequate, as the typical worst-case design would be inefficient and costly. Two-phase microchannel cooling, combining boiling heat transfer (utilizing the latent heat of vaporization) and a large surface area, offers the tantalizing potential of a highly efficient cooling solution [3]–[9].

However, two-phase cooling systems are prone to various flow boiling instabilities. Flow oscillations may trigger severe structural vibration, premature initiation of the critical heat flux condition, large wall thermal stress fluctuations, and harmful thermal fatigue [6], [10], [11]. Reduction or elimination of potential two-phase flow instabilities is a pre-requisite for the deployment of any two-phase cooling system [1]. Flow rate and temperature measurements offers the possibility of stable operation through feedback. However, the plant models are highly nonlinear and inaccurate. The performance of conventional model-based control (e.g., model predictive control) may suffer as a result.

This paper builds on our prior work on the modeling and control of microchannel flow instabilities [12]–[14] to include the evaporator wall temperature dynamics. The system is one-way coupled: flow dynamics affects the heat transfer coefficient, but the thermal subsystems does not affect the flow subsystem. The dependence of the heat transfer coefficient on the flow rate is highly nonlinear – low in the single phase region (vapor for low flow rate and liquid for high flow rate) and high in the two-phase region where the operation is desired. Furthermore, it also depends on the heat load and the flow rate. The challenge is to determine the optimal operating point without a precise model. Our approach is to first stabilize the flow subsystem and then adjust the flow rate to maximize the heat transfer coefficient for the optimal thermal system. We draw the inspiration from extremum seeking control, which is a long-established model-free method to adjust the input to adaptively seek out the maximum of some objective function [15]. In contrast to the standard extremum seeking formulation, we do not have the direct measurement of the performance index of interest, i.e., the heat transfer coefficient. Instead, we use the wall temperature measurement to first estimate the heat transfer coefficient and then adjust the flow rate in a simple hill-climbing algorithm.

In this paper, we first introduce the two-phase flow characteristics in microchannels. Next, we develop the dynamic thermal-fluid model of microchannels, in part based on the experimental oscillatory flow and thermal transient data. The main result of the paper is on flow stabilization and maximization of the heat transfer by adjusting the inlet flow rate based on the wall (electronics surface) temperature and flow rate measurements.

II. Two-Phase Flow Characteristics

To quantify flow boiling characteristics in uniformly heated channels, a lumped momentum balance is applied to two-phase flow in a horizontal channel

$$\frac{d\dot{m}}{dt} = \frac{A}{L}\left(\Delta P_S - \Delta P_D\right),\ \Delta P_S = P_0 - P_e \tag{1}$$

where $\dot{m}$ is the mass flow rate, ΔP_S is the supply pressure drop, P_0/P_e are the inlet/exit fluid pressures, and the demand

pressure drop, ΔP_D, includes both the acceleration and frictional pressure drops, and is dependent on the channel flow rate and imposed heat load.

A key attribute of a heat exchanger is its pressure-drop demand curve, characterized as a function of mass flow rate for constant heat flux (i.e., $\Delta P_D(\dot{m},q)$). When the flow rate is high, the flow is single-phase liquid. As the mass flow rate is reduced while other conditions are unchanged, boiling will commence. Further reduction in the flow rate will gradually cause vigorous boiling. Since frictional and acceleration pressure drops tend to increase as the void fraction (or flow quality, i.e., the portion of vapor in the two-phase mixture) increases, the pressure-drop will reach a minimum before starting to increase as flow rate continues to decrease. This region of negative slope in the demand curve, corresponding to the two-phase flow, is the key source of instability (and hence operation challenge) of two-phase heat transfer systems [11], [16].

For a constant supply pressure, (1) is first order and the flow stability is determined by the slope of the demand curve (this instability mechanism is known as the Ledinegg instability) [12]. In the presence of a compressible volume, the system dynamics becomes second order, and flow oscillation may occur (known as the pressure-drop instability) [13]. For multiple parallel channels, the individual channel flow may not be uniform (known as the parallel-channel flow maldistribution) [17], [18].

III. Thermal-Fluid Model

Large pressure-drop and thermal oscillations have been observed in several experimental studies due to the existence of appreciable compressibility in the two-phase flow loop [13], [14]. Flow oscillations can trigger thermal oscillations and transient burn-out in microchannels, and the large amplitude fluctuations in the microchannel wall temperature result in significant thermal stresses and harmful thermal fatigue. A pressure-drop flow oscillation model was developed in [13] to analyze the two-phase flow dynamics in microchannels. This paper focuses on the thermal oscillations which directly affect the transient cooling capacity and energy transport efficiency.

To characterize the compressible volume, an equivalent surge tank was assumed to be located upstream of the flow boiling channels as shown in Fig. 1. Moreover, two virtual restriction elements are used to represent the combined flow resistance from the supply pump to the main boiling branch and the surge tank. Notice that a lumped boiling channel has been used to represent the whole microchannel heat sink, since the experimental pressure fluctuations are measured between the inlet and outlet manifolds of the microchannel cold plate. As indicated in the flow loop [13], the microchannel flow meter is placed before the boiling channel in Fig. 1, because the pressure drop across the microchannel flow meter is significant in the experiments.

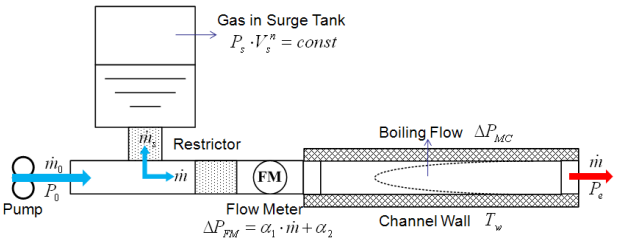

Fig. 1. Schematics of a boiling channel with an upstream surge tank

A. Pressure-Drop Oscillations

As shown in Fig. 1, the inlet mass flow rate of the overall system is $\dot{m}_0 = \dot{m} + \dot{m}_s$, where $\dot{m}$ is the flow rate in the boiling channel and $\dot{m}_s$ the flow rate into of the surge tank. In the tank, the gas is assumed to be inert and polytropic, thus, the pressure P_s and the gas volume V_s satisfy, $P_s \cdot V_s^n = constant$, where n is a fixed polytropic index of expansion. The volume change of the compressible gas in the surge tank is proportional to the upstream liquid inflow with density ρ_f, that is, $\dot{m}_s = -\rho_f \cdot dV_s/dt$. Note that the boiling channel exit pressure P_e and temperature are maintained at a constant value by an external temperature controller immersed in the downstream reservoir.

Combining mass balance with the momentum balance (1), the overall pressure-drop flow model may be written as [13]:

$$I\frac{d^2\dot{m}}{dt^2} + \frac{d(\Delta P_c)}{d\dot{m}}\frac{d\dot{m}}{dt} + C_s\dot{m} = C_s\dot{m}_0,\ C_s = \frac{nP_s}{\rho_f V_s} > 0 \qquad (2)$$

where the overall pressure drop, ΔP_c, in the main branch includes the pipe, flow meter (FM), and microchannel (MC) pressure drops, $\Delta P_c = \Delta P_r + \Delta P_{FM} + \Delta P_{MC}$, $\Delta P_r = \gamma \cdot \dot{m}$ is the pressure loss due to flow resistance upstream the flow meter, $\Delta P_{FM} = \alpha_1\dot{m} + \alpha_2$ is the flow meter pressure drop, and ΔP_{MC} is the microchannel pressure drop. We model the microchannel pressure drop as

$$\frac{d(\Delta P_{MC})}{d\dot{m}} = \delta\,(\dot{m} - \dot{m}_a)\,(\dot{m} - \dot{m}_b)\,. \qquad (3)$$

More complex model is possible, but this simple quadratic function captures the essence: The negative portion of the parabola, $\dot{m}_a < \dot{m} < \dot{m}_b$, corresponds to the two-phase flow exiting the evaporator, and the two positive ends of the parabola, $\dot{m} > \dot{m}_b$ and $\dot{m} < \dot{m}_a$ correspond for subcooled liquid and superheated vapor.

Using the experimental flow measurements in a microchannel heat exchanger testbed, a flow model has been identified [13]. The phase portrait of supply pressure drop vs. mass flow rate is shown in Fig. 2 indicating that the proposed model structure is able to capture the system-level dynamic flow oscillation pheonomenon.

B. Thermal Oscillations

To characterize thermal oscillations, the lumped energy balance approach is used to model the microchannel wall temperature dynamics:

$$C_{pw}\rho_w A_w L_w \frac{dT_w}{dt} = q - \alpha_w S_w\left(T_w - T_f\right) \qquad (4)$$

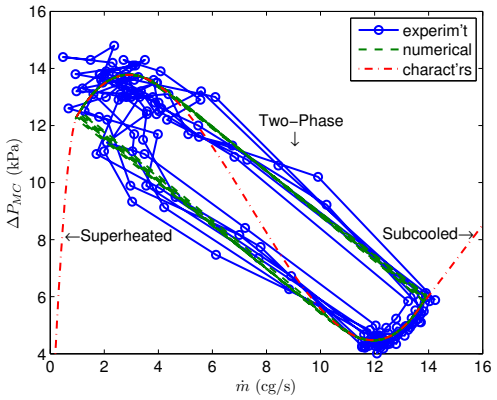

Fig. 2. Steady state flow characteristics and phase portrait comparison of pressure drop flow oscillation [13]

where $C_{pw}\rho_w A_w L_w$ is the microchannel wall thermal inertia, S_w the microchannel wall surface area, T_f the system fluid temperature (assumed to be constant in the two-phase regime, which follows from the assumption that P_e is constant), and q is the imposed heat load. By using the testbed parameters and transient wall temperature measurements, one can calculate the time-varying heat transfer coefficient (HTC), α_w, from (4), as shown in Fig. 3. To characterize the transient HTC, a correlation was developed in [14]:

$$\alpha_w = c_1 \cdot \mathrm{Bo}^{c_2} \cdot \mathrm{We}^{c_3} \cdot \Phi \cdot \frac{k_f}{D_h} \tag{5}$$

$$\mathrm{Bo} = \frac{Aq''}{\dot{m} \cdot h_{fg}},\ \mathrm{We} = \frac{\dot{m}^2 \cdot D_h}{A^2 \rho_f \cdot \sigma_f} \tag{6}$$

$$\log(\Phi) = c_4 \left(\frac{\dot{m}}{\dot{m}_0}\right)^3 + c_5 \left(\frac{\dot{m}}{\dot{m}_0}\right)^2 + c_6 \left(\frac{\dot{m}}{\dot{m}_0}\right) \tag{7}$$

where Φ is the two-phase heat transfer multiplier, and $c_i, i = 1,\ldots,5$, are the model parameters to be determined In this study, it is found that the effect of Weber number, *We*, is negligible. The heat transfer model validation/prediction result is illustrated in Fig. 3.

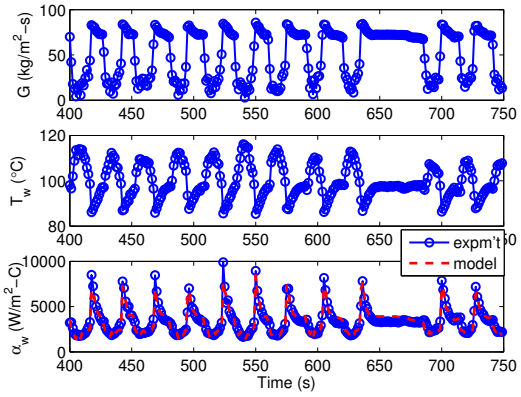

Fig. 3. Heat transfer coefficient comparison for oscillatory flows between experimental data and numerical calculation based on the identified correlation

C. Thermal-Fluid Modeling

The combined thermal-fluid model is of the following form:

$$\frac{d^2\dot{m}}{dt^2} + \frac{1}{I}\left[\frac{d\Delta P_{MC}}{d\dot{m}} + \alpha_1 + \gamma\right]\frac{d\dot{m}}{dt} + \frac{C_s}{I}(\dot{m} - \dot{m}_0) = 0 \tag{8}$$

$$I\frac{d\dot{m}}{dt} = \Delta P_{MC}^S - \Delta P_{MC}(\delta, \dot{m}_a, \dot{m}_b, e) \tag{9}$$

$$\beta C_{pw}\rho_w A_w L_w \frac{dT_w}{dt} = q - \alpha_w S_w \left(T_w - T_f\right) \tag{10}$$

where ΔP_{MC} is given by (3), e is the integration constant, and β represents the uncertainty in the microchannel wall thermal inertia and the potential thermal loss in the microchannel heat sink. The experimental testbed provides three sets of measurements: flow meter pressure drop ΔP_{FM}^E, microchannel pressure drop ΔP_{MC}^E, and microchannel wall temperature, T_w^E. In the thermal-fluid model, we select the parameters $(I, \delta, \dot{m}_a, \dot{m}_b, \gamma, C_s, e, \beta)$ to fit the model response to the experimental data (the rest of the parameters are obtained from direct physical measurements).

The comparison between experimental and simulation results is shown in Fig. 4 for the specified conditions (heat load $q = 60$W, pump voltage $U_p = 0.38$V). Two other independent data sets (with higher pump voltage, $U_p = 0.40$V and 0.42V, and higher inlet mass flow rate) are also used to evaluate the predictive capability of the model. As shown in Fig. 5, in both cases, the HTC prediction matches well with the experimental data. For the single-phase laminar flow, Nusselt number, Nu, is constant [5], [19]. With the thermal conductivity k_f, we can calculate HTC from $\alpha_w = \mathrm{Nu} \cdot k_f / D_h$ to assess our model quality for extrapolating the HTC prediction range. For saturated vapor flow, the HTC based on [5] is 1369W/m^2-C, while our HTC model prediction is about 1340W/m^2-C for very low mass flow rate. The available HTC correlation for subcooled flow can be used to build the global heat transfer characteristics. The full range of the heat transfer characteristics under both stable and oscillatory flow conditions is shown in Fig. 5.

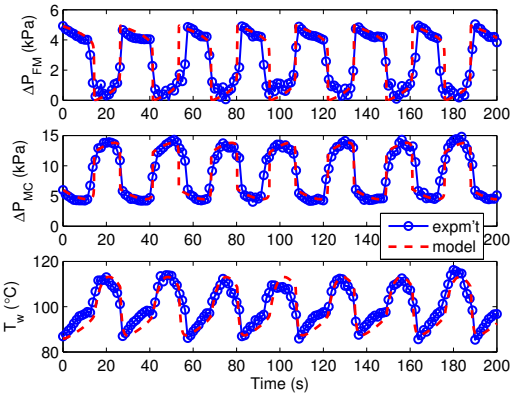

Fig. 4. Comparison between experimental data and identified model response for Flow meter (FM), microchannel (MC) pressure-drop, and wall temperature

Fig. 5 shows that the subcooled flow directly transitions

to film boiling [19] under relatively low flow rate. Once the flow rate is increased, nucleate/convective boiling becomes dominant, and the heat transfer performance is significantly enhanced. When the flow rate is further increased, the imposed heat load would not be enough to boil the fluid. Therefore, the heat transfer coefficient for single-phase liquid will decrease again since the thermal conductivity decreases with increasing flow rate for a fixed heat load. However, in the low-medium flow rate range, experimental data are limited because nucleate flow boiling is very sensitive to operating conditions, therefore large uncertainties are associated with the resulting boiling heat transfer model. In general, the nucleate or convective boiling has superior heat transfer performance, but it is very challenging to characterize accurately.

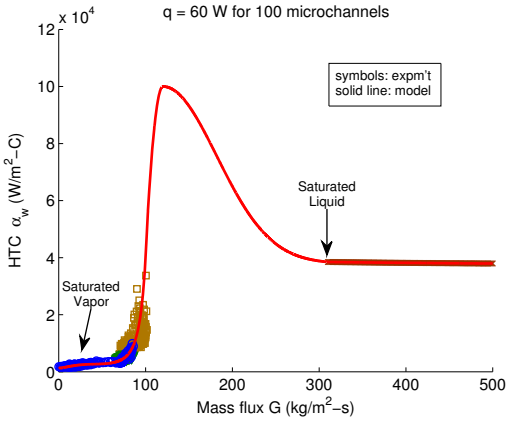

Fig. 5. Heat transfer characteristics (HTC, α_w, versus mass flux, $G = \dot{m}/A$). Symbols indicate experimentally obtained HTC values.

IV. Active Thermal-Fluid Control

The objective for an electronics cooling system involves optimal cooling performance (maximum heat removal subject to desired wall temperature) while minimizing the supply pump power for working fluid circulation. Although microchannel two-phase cooling can provide a promising solution, microchannel heat exchangers are prone to various boiling flow instabilities especially pressure-drop flow and thermal oscillations, which would lead to significant operational problems. We pose the active cooling objectives as: maintain stable two-phase flow, optimize transient cooling performance, maintain safe heat source (silicon) wall temperature, and minimize the supply pump power consumption.

A. Thermal-Fluid Control Model

Based on the boiling flow model (2) and the wall thermal model (4) with (5)-(7), the micro-thermal-fluid dynamics can be simulated to evaluate the active cooling performance of the designed control system. The pressure-drop flow oscillation model (2) may be written in the following state space form:

$$\begin{cases} \dot{x}_1 = x_2 \\ \dot{x}_2 = -d \cdot x_1 - f(x_1, q) \cdot x_2 + d \cdot u \end{cases} \tag{11}$$

where $x_1 = \dot{m}$, $d = C_s/I > 0$, and $f(\dot{m}, q)$ may be negative or positive corresponding to two-phase and single-phase flow regimes under a certain heat load q.

We write the thermal equation as

$$\dot{x}_3 = \kappa_1 \cdot q - \kappa_2 \cdot g(x_1, q) \cdot x_3 \tag{12}$$

where $x_3 = T_w - T_f$, $\kappa_1 = 1/I_w$, $\kappa_2 = S_w/I_w > 0$, and the heat transfer coefficient, $\alpha_w = g(x_1, q) > 0$.

The control objective is to choose u to stabilize the system (i.e., drive $\dot{x}_i$, $i = 1, \ldots, 3$, to zero) and maintain wall temperature below a specified level, $x_3 < x_{3_{\max}}$. The cooling performance of the system is typically given by the coefficient of performance (COP) based on the steady state operation:

$$\text{COP} = \frac{q}{x_1 \Delta P_c(x_1, q)/\rho_f} \tag{13}$$

where $\Delta P_c(x_1, q) = \Delta P_r(x_1) + \Delta P_{FM}(x_1) + \Delta P_{MC}(x_1, q)$. At the steady state, q is a function of (x_1, x_3) and satisfies the implicit equation

$$q = \frac{\kappa_2}{\kappa_1} g(x_1, q) x_3. \tag{14}$$

To find the optimal steady state flow rate, one would solve x_1 to maximize the COP (13) with $x_3 = x_{3_{\max}}$. However, the expressions for g and ΔP_{MC} are highly uncertain, hampering a direct static optimization approach. Instead, we will solve the suboptimal problem of first finding x_1 to maximize the HTC g for a given constant q. This would give the lowest achievable x_3. The procedure is repeated with the heat input q gradually increased until x_3 reaches $x_{3_{\max}}$. A separate flow stabilization loop will be used to achieve the required x_1 in this procedure. Since the dynamics of the thermal subsystem is typically much slower than the flow subsystem, the time scale separation would allow the two controllers to be combined to maintain the over system stability and performance (as in the backstepping approach [20]).

B. Thermal Control to Maximize HTC

We will first consider only the thermal control problem (12) with a constant (but unknown) q, x_1 as the control variable, and x_3 as the measured output. Our goal is to find x_1 to maximize $g(x_1, q)$, without the explicitly knowledge of g (the only property we assume is that g is positive and unimodal). This is a good candidate for the extremum seeking control, but g is not directly measurable. Therefore, we use an alternate method by first estimate g by using x_3 and the dynamics (12), and then apply a simple gradient hill climbing algorithm to maximize this estimated g. For a constant x_1, (12) is linear in two constant unknown parameters, q and g. This may be readily solved either in batch or recursive mode. We use the following simple strategy of converting the problem into a linear least square problem. First multiply both sides of (12) by x_3 to obtain

$$\frac{1}{2}\frac{d\left(x_3^2\right)}{dt} = \kappa_1 q x_3 - \kappa_2 g x_3^2. \tag{15}$$

Integrate both sides for one time period, from t_{k-1} to t_k. Then we have

$$\frac{1}{2}x_3^2(t_k) - x_3^2(t_{k-1}) = \kappa_1 q \int_{t_{k-1}}^{t_k} x_3(t)\,dt - \kappa_2 g \int_{t_{k-1}}^{t_k} x_3^2(t)\,dt. \tag{16}$$

Collecting the equations over multiple samples, one can direct solve for q and g.

To implement the hill climbing algorithm to maximize g, we use a simple finite difference estimate of $\frac{\partial g}{\partial x_1}$. The entire algorithm is summarized below:

1) Impose a positively-perturbed move x_{1_p} for a certain time interval, estimate the corresponding unknown g_p and q_p from the linear least square problem based on (16).
2) Impose a negatively-perturbed control move x_{1_n} for a certain time interval, estimate the corresponding unknown g_n and q_n from the linear least square problem based on (16).
3) Approximate the gradient of g by the finite difference:

$$\frac{\partial g}{\partial x_1} \approx \frac{g_p - g_n}{u_p - u_n}. \tag{17}$$

4) Apply the gradient algorithm to adjust x_1:

$$\Delta x_1 = \lambda \operatorname{sgn}\left(\frac{\partial g}{\partial x_1}\right). \tag{18}$$

5) Wait until the system reaches a steady state, then repeat Step 1.

The application of the above algorithm is illustrated in Fig. 6. Note that the estimates for the constant heat load and HTC in each identification/gradient-update step follows closely the actual parameters used, as shown in Fig. 7. The wall temperature continues to decrease until the heat transfer coefficient reaches its maximum. Note that the physical modeling from the previous section is only used in simulation but not in the controller implementation.

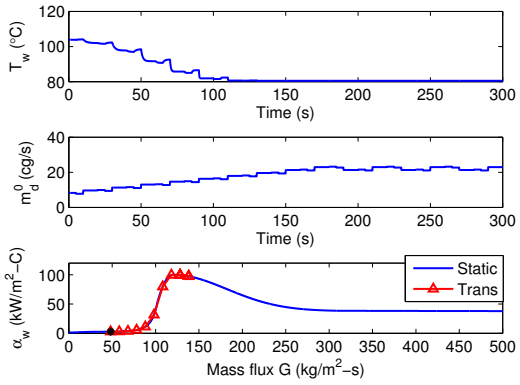

Fig. 6. Extremum seeking thermal control (m_d^0: mass flow rate used as the input)

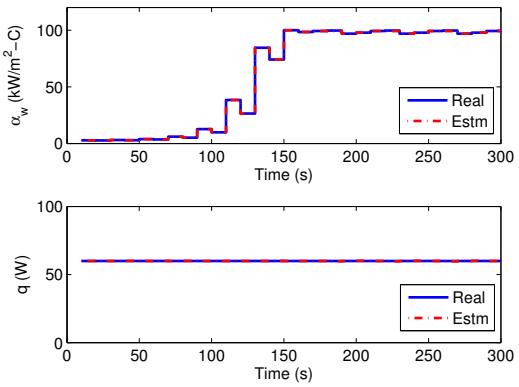

Fig. 7. Estimation of the heat transfer coefficient and heat load in extremum seeking thermal control

C. Cascade Micro-Thermal-Fluid Control

In the section above, only thermal control is considered. In the two-phase regime, the flow system itself may be unstable. We propose a cascade thermal-fluid control architecture where the inner flow controller is used for flow stabilization, and the outer extremum-seeking thermal controller is used to achieve the best cooling performance:

$$u = \dot{m}_0 = u_f + u_t. \tag{19}$$

We use a simple derivative controller for flow stabilization, $u_f = -K\frac{d\dot{m}}{dt}$, and for the outer loop u_t, we replace x_1 in the extremum seeking thermal controller with u (since at steady flow, $x_1 = u$).

In the simulation study, we choose $t_s = 0.1$ and $N = 50$ (number of samples used for the identification of q and g) and a simple flow stabilizing control law, $u_f = -15.93\dot{x}_1/d$. The thermal controller u_t is employed to maintain the microchannel wall temperature below its safe operation limit of 85°C. Note that although the flow acceleration $\dot{x}_1 = d\dot{m}/dt$ is usually unavailable, it is straightforward to implement a state estimator based on the mass flow rate measurement [13]. The closed-loop cascade control simulation in Fig. 8 show both flow stabilization and HTC maximization as desired. Note that the HTC is driven from initial low level to the maximum. Further stability analysis is underway to rigorously justify the stability and performance of the combined system using singular perturbation.

V. Concluding Remarks

For microchannel-based cooling of high power electronic devices, conventional controllers such as proportion-integral control are not sufficient to address the variations in the heat transfer coefficients under different operating conditions. Model-based control and optimization using analytical expression of the heat transfer coefficient may be appealing but is not a reliable approach due to the large uncertainties in the boiling heat transfer model, especially in the desired nucleate/convective boiling region. In this study, we developed an extremum-seeking control scheme to maximize the heat

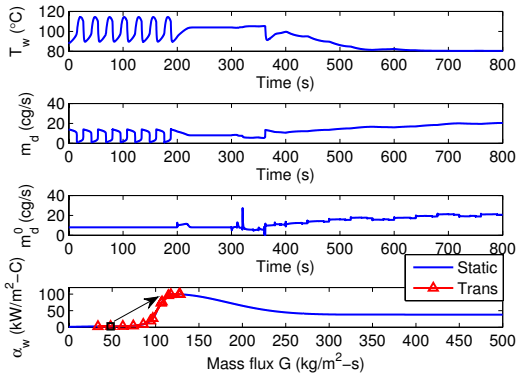

Fig. 8. Cascade extremum-seeking thermal-fluid control combining flow stabilization with extremum seeking thermal control (m_d^0: input mass flow controlled by pump)

transfer coefficient without using an accurate heat transfer model. This scheme is then combined with a flow controller to achieve both flow stabilization and optimized thermal performance. We are currently investigating the performance in the oscillatory flow regime for transient heat loads.

VI. Acknowledgment

This work is supported in part by the Office of Naval Research (ONR) under the Multidisciplinary University Research Initiative (MURI) Award N00014-07-1-0723 entitled "System-Level Approach for Multi-Phase, Nanotechnology-Enhanced Cooling of High-Power Microelectronic Systems," and in part by the Center for Automation Technologies and Systems (CATS) under a block grant from the New York State Foundation for Science, Technology and Innovation (NYSTAR). The authors would like to thank Tao Tong, Je-Young Chang, Ravi Prasher in the Intel Corporation for providing experimental transient data.

References

[1] S. V. Garimella, A. S. Fleischer, et al., "Thermal challenges in next-generation electronic systems", *IEEE Transactions on Components and Packaging Technologies*, vol.31, pp.801-815, 2008.

[2] T. W. Webb, T. M. Kiehne, and S. T. Haag, "System-level thermal management of pulsed loads on an all-electric ship", *IEEE Transactions on Magnetics*, vol.43, pp.469-473, 2007.

[3] S. G. Kandlikar and A. V. Bapat, "Evaluation of jet impingement, spray and microchannel chip cooling options for high heat flux removal", *Heat Transfer Engineering*, vol.28, pp.911-923, 2007.

[4] J. Lee and I. Mudawar, "Low-temperature two-phase microchannel cooling for high-heat-flux thermal management of defense electronics", *IEEE Transactions on Components and Packaging Technologies*, vol.32, pp.453-465, 2009.

[5] S. G. Kandlikar, S. Garimella, D. Li, et al., *Heat Transfer and Fluid Flow in Minichannels and Microchannels*, Elsevier, 2006.

[6] J. R. Thome, "State-of-the-art overview of boiling and two-phase flows in microchannels", *Heat Transfer Engineering*, vol.27, pp.4-19, 2006.

[7] L. Zhang, J.-M. Koo, L. Jiang, et al., "Measurements and modeling of two-phase flow in microchannels with nearly constant heat flux boundary conditions", *IEEE/ASME Journal of Microelectromechanical Systems*, vol.11, no.1, pp.12-19, 2002.

[8] C.-J. Kuo, A. Kosar, Y. Peles, et al., "Bubble dynamics during boiling in enhanced surface microchannels", *IEEE/ASME Journal of Microelectromechanical Systems*, vol.15, no.6, pp.1514-1527, 2006.

[9] C.-J. Kuo and Y. Peles, "Pressure effects on flow boiling instabilities in parallel microchannels", *International Journal of Heat and Mass Transfer*, vol.52, pp.271-280, 2009.

[10] A. E. Bergles, J. H. Lienhard, G. E. Kendall, P. Griffith, "Boiling and evaporation in small diameter channels", *Heat Transfer Engineering*, vol.24, pp.1840, 2003.

[11] S. Kakac and B. Bon, "A review of two-phase flow dynamic instabilities in tube boiling system", *International Journal of Heat and Mass Transfer*, vol.51, pp.399-433, 2008.

[12] T. J. Zhang, T. Tong, Y. Peles, R. Prasher, et al., "Ledinegg instability in microchannels", *International Journal of Heat and Mass Transfer*, vol.52, pp.5661-5674, 2009.

[13] T. J. Zhang, Y. Peles, J. T. Wen, et al., control of pressure-drop flow instabilities in boiling microchannel systems", *International Journal of Heat and Mass Transfer*, vol.53, pp.2347-2360, May, 2010.

[14] T. J. Zhang, J. T. Wen, Y. Peles, et al., "Micro-thermal-fluid transient analysis and active control for two-phase microelectronics cooling", in *Proceedings of the 6th IEEE Conference on Automation Science and Engineering (CASE 2010)*, Toronto, Canada, August 21-24, 2010.

[15] K. B. Ariyur and M. Krstic, *Real-Time Optimization by Extremum Seeking Control*, Wiley & Sons, Inc., 2003.

[16] J. Yin, *Modeling and Analysis of Multiphase Flow Instabilities*, PhD Thesis, Rensselaer Polytechnic Institute, 2004.

[17] J. Xu, J. Zhou, and Y. Gan, "Static and dynamic flow instability of a parallel microchannel heat sink at high heat fluxes", *Energy Conversion and Management*, vol.46, pp.313-334, 2005.

[18] T. J. Zhang, J. T. Wen, A. Julius, et al., "Parallel-channel flow instabilities and active control schemes in two-phase microchannel heat exchanger systems", in *Proceedings of the 2010 American Control Conference (ACC 2010)*, Baltimore, MD, July, 2010.

[19] V. P. Carey, *Liquid-Vapor Phase-Change Phenomena: An Introduction to The Thermophysics of Vaporization and Condensation Processes in Heat Transfer Equipment, second ed.*, Taylor & Francis, 2008.

[20] H. K. Khalil, *Nonlinear Systems, 3rd ed.*, Prentice Hall, Upper Saddle River, N.J., 2002.